

# Blind Background Removal in Dental Panoramic X-ray Images: An Application Approach.

Peter Michael Goebel<sup>1,2</sup>, Nabil Ahmed Belbachir<sup>1</sup> and Michael Truppe<sup>3</sup>

<sup>1</sup> Vienna University of Technology, Institute of Computer Aided Automation, Pattern Recognition and Image Processing Group, Favoritenstr. 9/183-2, 1040 Vienna, Austria.  
Tel: 00431-58801 18351, Fax: 00431-58801 18392, Email: <nabil,goe>@prip.tuwien.ac.at

<sup>2</sup> fh-campus wien, Technical Project- and Processmanagement, 1100 Vienna, Austria.

<sup>3</sup> Karl Landsteiner Institute for Biotelematics, Danube University, 3500 Krems, Austria.

Tel: 00432742-258 958 32, Fax: 00432742-258 958 31, Email: mtruppe@bioelematics.at

**Key words:** Medical and Biomedical Imaging, Image Analysis

- 1. What is the original contribution of this work?** In this paper, a dedicated approach based on A-trous wavelet transform, which operates completely blind, for background removal in dental panoramic X-ray images is presented.
- 2. Why should this contribution be considered important?** After the background preprocessing, the remaining components are coherent noise and diagnostic information. The advantage in using the wavelet domain is that the background noise is removed using an appropriate estimation of the different energy contributions at different scales and locations.
- 3. What is the most closely related work by others and how does this work differ?** The most closely work is those of reference [12, 13]. In addition to background removal in X-ray images, the proposed new approach also removes unwanted modulation in the image of interest.
- 4. How can other researchers make use of the results of this work?** For dental panoramic X-ray image denoising, with respect to coherent noise, an artificial spatial noise map model can be parameterized, which can be thought as a one-to-one realization of any type of noise (additive or multiplicative as well) within the original image. Thus, the proposed method can be used to tract this noise estimate as another form of background and subtract it from the original image.
- 5. Has this work been presented/submitted elsewhere?** No.
- 6. Which form of presentation is preferred: Oral or Poster?** Oral.

# Blind Background Removal in Dental Panoramic X-ray Images: An Application Approach.

Peter Michael Goebel<sup>1,2</sup>, Nabil Ahmed Belbachir<sup>1</sup> and Michael Truppe<sup>3</sup>

<sup>1</sup> Vienna University of Technology, Institute of Computer Aided Automation, Pattern Recognition and Image Processing Group, 1040 Vienna, A.

<sup>2</sup> fh-campus wien, Technical Project- and Processmanagement, 1100 Vienna, A.

<sup>3</sup> Karl Landsteiner Institute for Biotelematics, Danube University, 3500 Krems, A.

**Abstract.** Dental Panoramic X-ray images are images with complex content, because several layers of tissue, bone, fat, etc. are superimposed. Non-uniform illumination, stem from the X-ray source, gives extra modulation to the image, which causes spatially varying X-ray photon density. The interaction of the X-ray photons with the density of matter causes spatially coherent varying noise contribution. Many algorithms exist to compensate background effects, by pixel based or global methods. However, if the image is contaminated by a non-negligible amount of noise, that is usually non-Gaussian, the methods cannot approximate the background efficiently.

In this paper, a dedicated approach is presented, which operates completely blind<sup>4</sup>, using the A-Trous multiresolution transform to alleviate this problem. The new method estimates the background bias from a reference scan, which is taken without a patient. Then the energy of the background estimate is subtracted from the energy of the mixture, using the properties of the wavelet decorrelation between useful information and noise. The advantage in using the wavelet domain is that the background noise is removed using an appropriate estimation of the different energy contributions at different scales and locations. After the background preprocessing, only two components remain, coherent noise and diagnostic information. Finally, a comparison to a standard denoising method is given. This approach has been tested on 200 samples from a database of panoramic X-ray images where the results are cross validated by medical experts. . . .

## 1 INTRODUCTION

Non-uniform illumination of any kind generates non-uniform background in an image. The term background comes from the usual classification of the image data into regions of interest and unwanted regions, referred foreground and background, respectively [10].

---

<sup>4</sup> It means the separation of a set of independent signals from a set of mixed signals, without the aid, or only little, of information about the nature of the signals.

## 1.1 Background Removal Methods

There are pixel based methods (e.g. Kalman filtration [8], Adaptive Thresholding [9]); global methods which generate the rules for the adaption of the background estimate from some measurable image attributes and also non-parametric models [7].

A polynomial fit to a number of points associated with the background is usual when the non-uniformity is additive, and the resulting polynomial surface is subtracted from the whole image. If the non-uniformity is multiplicative, a correction image is generated, corresponding to the polynomial surface and used to scale the original image. The pixels of this correction image contain a factor that represents how many times brighter the non-uniform image is than the uniform image at that point.

Sometimes, a different definition exists, of what the background is: in [13] the background is meant to be the 'bright' surrounding area on a X-ray film viewing box, where the diagnostic film is smaller than the viewing box, thus the surrounding, bright white area has physiological influence on the detectability of contrast details in the darker X-ray film area [2]. The algorithm builds up a probabilistic model and cuts out the radiography by the biggest gradient at its border. The proposed, new approach is different, because it removes unwanted modulation in the image of interest, too.

## 1.2 Basics of Panoramic Radiography

Dental Panoramic Radiography (DPR) is a technique where the entire dentition is projected onto a sensing device. The physics of such a radiographic process can be subdivided into X-ray source, interaction of the beam with matter and imaging of the remaining photons. Source and detector are in opposition, rotated around the patient's head. The focal area of the X-ray beam describes a planar curve, which is standardized for the human teeth and jaws.

The photon attenuation of each type of matter depends on its elementary and chemical composition as well as the beam. This effect is quantified by the linear mass attenuation coefficient, which gives the fraction of photons that are absorbed by unit thickness of matter [6], which is not a constant and varies by photoelectric absorption, coherent scatter and Compton scatter [1].

## 1.3 Image Degradation

Only photons absorbed by matter generate good image contrast. During a DPR scan of the entire dentition, the photon rate has to be increased, when the X-ray beam crosses bones from the spine region. Thus a non-uniform illumination of the radiograph is caused, leading to additional, spurious modulation of the image.

## 2 THE METHOD EXPLAINED

As the geometry of the DPR system is fixed, a scan, taken without a patient can provide a good estimate for the background. Unfortunately, subtracting a background estimate directly from the diagnostic image usually increases the noise contribution in the difference image, because noise cannot be subtracted from noise in the spatial domain.

Therefore, it is more convenient to perform this subtraction in another domain, by decomposing the image into different contributions in several frequency bands and at different scales, forming a undecimated, over complete representation, namely by the A-Trous multi resolution transform [5].

### 2.1 Image Model

The X-ray generator in Figure 1 produces photons with Poisson count statistic; the arrival-time difference between successive Poisson counts is Gamma distributed; the photons, with intensity  $I_0$ , travel through collimator and filter to the patient. Thus, the intensity  $I_1$  can be measured as it is proportional to the photon input energy to the patient. This photon energy interacts with the different layers of matter of the patient, therefore one can measure  $I_2$  at the sensor.

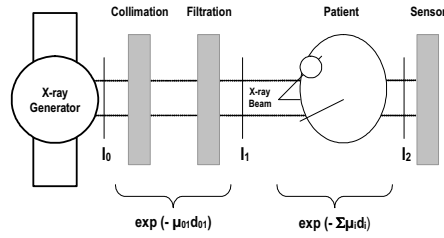


Fig. 1. Outline of the X-ray Physics.

Formulating the physical situation of Figure 1 in mathematical terms of linear attenuation coefficients leads to:

$$I_2 = I_0 \cdot \underbrace{\exp(-\mu_0 d_0)}_{\text{background scatter}} \cdot \underbrace{\exp\left(-\sum_{i=1}^K \mu_i d_i\right)}_{\text{diagnostic scatter}} \quad (1)$$

$I_1$

In (1) the intensity  $I_2$  at the sensor is decomposed into the background part  $I_1$ , which is further attenuated by the diagnostic part.

Photoelectric absorption and Compton scattering, as the main contributors for scattering the beam, induce the contrast function of matter, which forms the image. Unfortunately they produce also an amount of non-negligible noise. The statistic is quite non-Gaussian [4].

Since the exposure time is long (about 13 seconds for an entire panoramic scan), photon counts get quite high, thus stressing the central limit theorem, one can argue that for each exponential term in (1) the contribution of noise is given by an additive term of locally Gaussian noise, scaled by a spatially dependent, hidden factor  $\xi$ .

The hidden factor  $\xi$  incorporates the adaption close to the real statistic. Therefore the following approximation holds:

$$\begin{aligned} \widehat{Z}_{x,y}(I_2) &= \underbrace{Z_{x,y}}_{\text{image}} + \underbrace{\xi_{x,y}^{(1)} N_{x,y}(\overline{m}, \overline{\sigma})}_{\text{noise}} + \\ &\quad \underbrace{\hspace{10em}}_{\text{diagnostic mixture}} \\ &+ \underbrace{B_{x,y}}_{\text{illumination}} + \underbrace{\xi_{x,y}^{(2)} N_{x,y}(\overline{m}, \overline{\sigma})}_{\text{noise}} \\ &\quad \underbrace{\hspace{10em}}_{\text{background mixture}} \end{aligned} \quad (2)$$

In(2),  $\widehat{Z}_{x,y}$  is the output image, generated by  $I_2$  following (1), decomposed into the diagnostic mixture and the background mixture. Both mixtures are subdivided into an deterministic part and an additive random part. As explained above, the random parts have locally Gaussian statistic with a scale factor  $\xi^{(n)}$ .

## 2.2 Shrinking Method for the Wavelet Coefficients by Preservation of Energy

The idea is, that the energies of the contributions from the background illumination and the diagnostic information sum up to the mixture energy. Stressing Plancherel's Theorem [11] for non-ortho-gonal discrete wavelets and  $M < \infty$  finite scales, using the  $L^2(\mathfrak{R})$  norm, yields to (3):

$$E = \int \|s\|^2 = C_E \underbrace{\sum_{i=0}^{M-1} \frac{1}{2^i} \|w_i\|^2}_{\text{coefficients energy}} + \underbrace{\frac{1}{2^M} \|r_M\|^2}_{\text{resid. energy}} \quad (3)$$

where  $\int \|s\|^2$  is the signal energy in the spatial domain,  $w_i$  are the wavelet coefficients of the  $i^{\text{th}}$  scale and  $r_M$  is the residual scale. The constant  $C_E$  in (3) is chosen for conservation of energy and is determined for  $M=1$  and an input impulse function  $s = \delta$ , getting  $\|s\| = 1$  (see [11] for more details).

Calculating the energies, using (3), for the background estimate ( $E_B$ ), the output mixture image ( $E_{\widehat{Z}}$ ) and making up the balance by the norm of the energies, leads to the energy of the diagnostic mixture ( $E_D$ ) with background removed:

$$\|E_{D_{x,y}}\| = \left\| E_{\widehat{Z}_{x,y}} \right\| - \|E_{B_{x,y}}\| \quad (4)$$

From the reconstructed energy  $E_D$ , shrinkage weighting factors are introduced, to be able to convey the result to the coefficients:

$$f_{D_{x,y}} = \frac{\|E_{D_{x,y}}\|}{\|E_{\hat{Z}_{x,y}}\|} \dots \left\{ \frac{\|E_{\hat{Z}_{x,y}}\| > 0 : f_{D_{x,y}}}{0} \right\} \quad (5)$$

The corrected coefficients are calculated now, by application of the shrinkage weights:

$$\check{w}_{i_{x,y}} = w_{i_{x,y}} \cdot f_{D_{x,y}} \quad (6)$$

Then, the usually reconstruction of the A-Trous multiresolution transform yields to the reconstructed image  $I_R$ :

$$I_R = \sum_{i=0}^{M-1} \check{w}_i + r_M \quad (7)$$

To illustrate the method, consider three images, one image with gently inclining gray level ramp surface, as diagnostic image. Another image with a gray level checkerboard as the illuminating background, which is corrupted with two instances of Poisson noise. The ramp image and one of the corrupted checker-

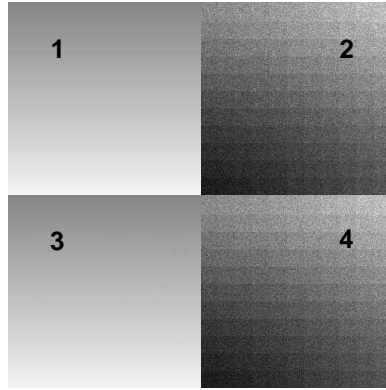


**Fig. 2.** Simulation of the method.

boards are mixed, while the other checkerboard image acts as the background estimate.

Figure-2 shows the experiment, the images with (label1) and (label2) are added and the method reconstructed the gray ramp image and as a cross validation, the gray ramp image (label1) is subtracted also from the mixture, that result shows (label4). From this experiment it is obvious, the method properly distinguishes the two images, including the noise contribution of the gray checkerboard image.

### 3 ANALYSIS AND RESULTS

In this section the results are shown of a 5-layer test phantom for digital dental x-ray systems [Quart (Ltd.), Germany, 2004]. The phantom is put in place of the patient's jaw.



**Fig. 3.** Background image estimate.

Figure-3 shows the background estimate, where one can see the non-uniformity of the X-ray illumination. Figure-4 shows the phantom image as the diagnostic mixture. First the background estimate is registered with the diagnostic image, then both images are transformed into the multiresolution domain. The algorithm, explained in section 2 is applied, by using  $M = 4$  scales and the standard triangle wavelet. Figure-5 shows the reconstruction after application of the method. A more detailed view is given in Figure-6. For comparison, it shows the result of a spatial background subtraction at a) and the result of the application of a standard stationary wavelet (SWT) denoising by a Daubechies wavelet db3, soft thresholding [3] at 3 scales in c). The original image is shown at quadrant b) and the result of the new method is found at d).

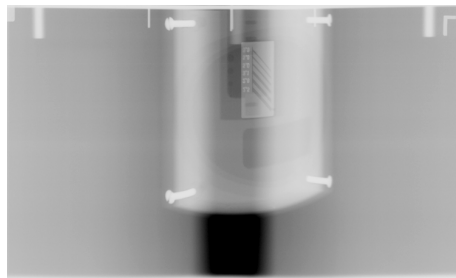


**Fig. 4.** Phantom diagnostic image mixture.



**Fig. 5.** Reconstruction of the phantom image.

## 4 CONCLUSIONS

In this paper, a new method for the estimation and removal of background in dental panoramic X-ray, by shrinking the wavelet coefficients under the constraint of preservation of energy, is given. The energy of an image, representing a background estimate, taken without a patient, is subtracted from the diagnostic image in the multiresolution domain.

The new method is compared to a spatial background subtraction method and to a standard denoising method, in fact the results show improved quality in either case. Main purpose of the new background subtraction method is not in denoising, but it is shown, that the background noise part is properly removed, without any need to choose parameters, thus the method is non-parametric.

As the method leave the part of noise unaffected, which is not found in the background, it can be the first stage of an improved denoising method, which consider the diagnostic noise part better. As proposed herein at first remove the background, then estimate a noise map of the remaining diagnostic noise and correct the factors (5) to remove the rest of the noise from the image. The advantage would be a better preservation of high frequency information such as fine, weak details within the image.

## References

1. Aird EGA. Basic Physics for Medical Imaging. Heinemann, Oxford, 1988
2. P. G. J. Barten. Physical model for the Contrast Sensitivity of the human eye. Proc. SPIE 1666, pp. 57-72 (1992)
3. D.L. Donoho. Denoising by Soft-thresholding. IEEE Trans. on Information Theory, Vol.41, pp.613-627, 1995
4. P.M. Goebel, A. N. Belbachir, M. Truppe. An application analysis approach for noise estimation in panoramic X-ray images. Proc. Joint Hungarian-Austrian Conf. Image Proc. and Pattern Recogn., HACIPPR 2005, Veszprém, Hungary, 11-13 May, 2005
5. M. Holschneider, R. Kronland-Martinet, J. Morlet, and Ph. Tchamitchian. A real-time algorithm for signal analysis with help of the wavelet transform. Wavelets,



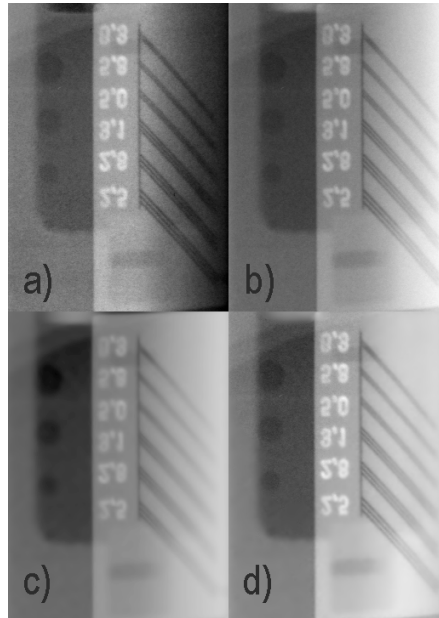


**Fig. 6.** A more detailed view of the results.

- Time-Frequency Methods and Phase Space, J. M. Combes, A. Grossmann, and Ph. Tchamitchian, Eds. Berlin: Springer, IPTI, 1989, pp. 286-297.
6. J. H. Hubbell, S. M. Seltzer Tables of X-Ray Mass Attenuation Coefficients and Mass Energy-Absorption Coefficients (version 1.4). NISTIR 5632, National Institute of Standards and Technology, Gaithersburg, MD (1995).
  7. W. Long and Yee-Hong Yang. Stationary background generation: an alternative to the difference of two images. *Pattern Recogn.*, **23**(12):1351-1359, 1990.
  8. C. Ridder, O. Munkelt, H. Kirchner. Adaptive Background Estimation and Foreground Detection using Kalman-Filtering. *Proc. Int. Conf. on recent Advances in Mechatronics ICRAM'95*, UNESCO Chair on Mechatronics, 193-199, 1995.
  9. A. E. Savakis Adaptive document image thresholding using foreground and background clustering. 1998 International Conference on Image Processing (ICIP '98) October 04-07, 1998.
  10. A. J. Shelley, N. L. Seed. Approaches to Static Background Identification and Removal. *Journal of the Institution of Electrical Engineers, IEE*, 1993.
  11. M. J. Shensha. Discrete Inverses for Nonorthogonal Wavelet Transforms. *IEEE Transactions on Signal Processing*, vol. **44**, no. 4, pp. 798-807, April 1996.
  12. T. M. Su and J. S. Hu. Background Removal in Vision Servo System Using Gaussian Mixture Model Framework. *IEEE Proc. on Int. Conf. on Networking, Sensing and Control*, Taipei, Taiwan, 2004.
  13. J. Zhang and H. K. Huang. Automatic Background Recognition and Removal (ABRR) in Computed Radiography Images. *IEEE Trans. on Medical Imaging*, Vol. **16**., No. 6., December 1997.